Desalination and Water Treatment
www.deswater.com
doi: 10.5004/dwt.2022.29109

279 (2022) 203–211
December

Identification of the rheological behavior of a thermoplastic polymer

Kamel Berkache[a,*], Zineeddine Louna[a], Abdelkader HadjSadok[b]

[a]*LMFTA, Faculty of Physics, USTHB, BP32 El-Alia, 16111 Bab-Ezzouar, Algiers, Algeria, email: kberkache@usthb.dz (K. Berkache)*
[b]*LAFPC, Saad Dahleb University, BP 270 Soumaa road, 09000 Blida, Algeria*

Received 28 June 2022; Accepted 5 October 2022

ABSTRACT

This work focused on a study of the rheological properties of Carbopol 990 microgel suspensions. Carbopol belongs to a family of highly cross-linked polymers which has attracted the attention of many rheologists. It has been used in a wide variety of rheological experiments as a model fluid. There is a need to understand how the overall rheological behavior of Carbopol 990 relates to the proposed models of its mesostructure. The changes in the rheological parameters of Carbopol 990 were investigated at various pH, concentrations and temperatures by using an MCR 302 rheometer which allowed for the modeling and identification of the behavior law that best described the hydrogel in comparison with existing reports.

Keywords: Rheology; Hydrogel; Viscoelasticity; Yield stress

1. Introduction

Complex fluids include a wide range of materials which exhibit unusual responses to external stresses. Their viscosities depend on the nature of the stresses applied. Some fluids thicken considerably under applied stresses, while others flow more freely. Materials like colloidal suspensions, foams, emulsions, granular materials flow irreversibly only if a certain stress value inside these materials, known as yield stress, is reached [1–9]. Carbopol is a family of commercial polymers frequently used in the cosmetics, pharmaceutical, paint and food industries as thickening, suspending, dispersing and stabilizing agents [10]. These polymers can be subdivided into several categories based on their physical structure and chemical composition, density and type of crosslinking, polymerization solvent, lattice electrical charge and physical appearance [11]. Carbopol is a very high molecular weight, hydrophilic and cross-linked polyacrylic acid polymer. This physical hydrogel presents a three-dimensional polymer network that is swollen by water and has entanglements between temporary and reversible polymer chains.

In the current investigation, Carbopol 990 was employed which exhibited high suspending, thickening and stabilizing capacity at low dosage. When neutralized with a base such as sodium hydroxide (NaOH), the polymer exhibited the ability to absorb and retain water. Polymer chains interconnected by crosslinks begin to hydrate and partially unwind to form irreversible agglomerates [12]. Carbopol 990 was supplied as a white, dry powder of primary particles with an average diameter of 0.2 μm. The rheological properties of Carbopol dispersions have been extensively studied [13–17]. These properties depended on the type and degree of cross-linking, which in turn depended on the swelling of the molecules and the average density. The Carbopol dispersion was generally considered as a simple model of yield stress fluids [18,19]. Their viscoplastic behavior at steady state was well represented by the Herschel–Bulkley model. However, Ketz et al. [20] argued that, for low stresses, microgels do not move relative to each other, but are able to deform, resulting

* Corresponding author.

Presented at the First International Congress of Energy and Industrial Process Engineering (ICEIPE'22) 23–25 May 2022, Algiers, Algeria

in solid-like elastic behavior. For high stresses there was a relative mobility of the microgels, leading to a liquid-like viscoelastic behavior. The aim was to identify the rheological properties of Carbopol 990 dispersions in different formulations at various polymer concentrations, pH values, and gel temperatures. Systematic, steady-state rheological experiments were performed.

2. Experimental

2.1. Test fluid

Carbopol is a water-soluble polymer that is available in different grades, usually supplied as a very light, low-density powder (Fig. 1a). It tends to float when added to water, requiring vigorous agitation. It is a cross-linked polyacrylate polymer, with an average molecular mass of 2.1×10^6 g/mol. The molecular chains have an average size of 2–7 microns (Fig. 1b). Direct cryo-scanning electron microscopy (cryo-SEM) imaging provided three-dimensional topographic contrast of polymer hydrogels made of different compositions.

This structure appeared either by increasing the polymer (concentration) or by neutralizing agent content. At a very low polymer concentration (C_{wt} = 0.1%), very fine fibers were formed and physically entangled (Fig. 2a). As the polymer concentration increased (Fig. 2a–c), the crosslink density increased, and subsequently, the polymer hydrogel formed the honeycomb structure possessing a wall.

2.2. Sample preparation

To produce the stock solution, the Carbopol 990 powder was slowly dispersed in distilled water. This was done by creating a gentle vortex in a 1,000 mL beaker with a large magnetic stir bar on a stir plate. The powder was added in small increments in the center of the vortex. Concentration was determined in percent mass by volume and the dry Carbopol was carefully weighed in an electronic balance before being added. Then the initial volume was fractionated and diluted with distilled water to obtain a range of concentrations. Fifteen mass concentrations were made ranging from C_{wt} = 0.02% to C_{wt} = 2%. After being assured that the polymers were sufficiently hydrated, as confirmed by the absence of visible conglomerates, the titration was started with NaOH. The samples were neutralized (pH ≈ 7). Then, several samples were prepared with the same mass concentration C_{wt} = 1% from the stock solution using a 10% NaOH solution by mass to titrate the samples. Small amounts of NaOH were added with a pipette, and then the samples were gently vortexed and allowed to equilibrate. A pH range was obtained from that of the unmodified pH sample, which was around 3.68, to a pH of 13.37. The pH meter essentially measured the chemical potential of H^+ which at equilibrium was the same in the gel as in the external solution [22]. The neutralization and the increase in pH was accompanied by a gelation process. Gelification consisted of an aggregation of dimers (up to four chains per junction), which themselves formed a three-dimensional network.

2.3. Measuring device

For polymeric solutions in a concentrated medium, rheological measurements were carried out using an Anton Paar MCR 302 rheometer of the cone-plane type, 60 mm in diameter (Fig. 3). The sample was placed between a plate and a cone of radius R, the axis of rotation of the cone was

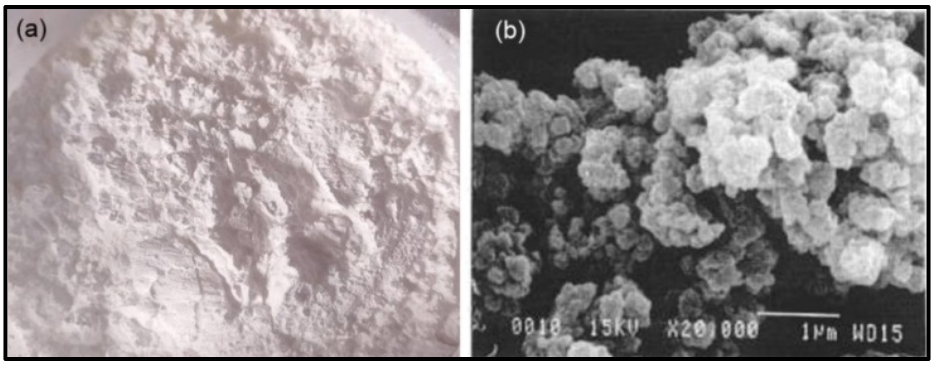

Fig. 1. Carbopol powder: (a) scanning electron micrograph of Carbopol resin ×20,000 and (b) white bar measures 1 μm [21].

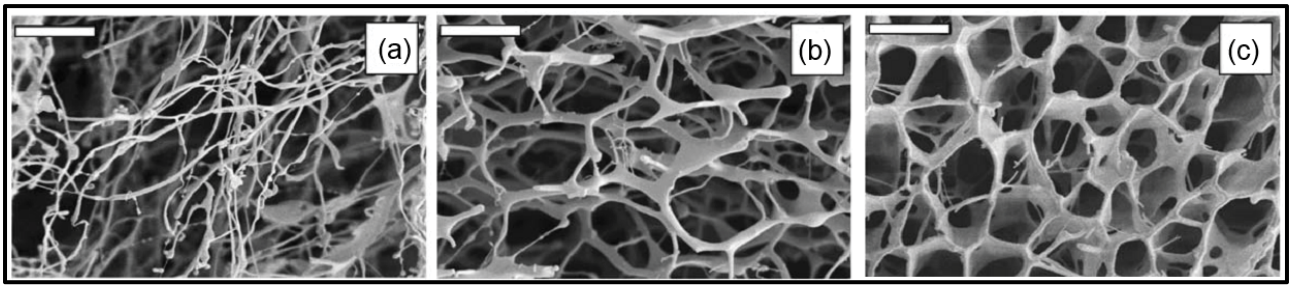

Fig. 2. Representative cryo-SEM images ×5,000 of samples at 25°C with: C_{wt} = 0.1% (a), C_{wt} = 2% (b), and C_{wt} = 4% (c) [14].

perpendicular to the plane of the plate. The generatrix of the cone made an angle with the plane of the plate. The end of the cone was truncated to separate the cone and the plane by a constant distance ("gap") of the order of a micrometer. This gap must be precisely maintained so as not to interfere with the conical symmetry of the module. The plate was fixed; on the other hand, the cone was subjected to a torque which caused a shearing movement by rotation.

3. Results and discussion

By examining the dependence of physical quantities on pH and concentration in addition to temperature, the aim was to derive conclusions about the underlying structure of Carbopol microgels based on steady-state measurements such as; characteristics of behavior near yield stress observed in flow curves and plots of viscosity and stress vs. shear rate.

3.1. Rheological characterization

It has recently been shown that even in the case of a Carbopol gel, the solid-fluid transition does not occur at a well-defined value of the applied stress but gradually [12–27]. Moreover, the Herschel–Bulkley constitutive relation cannot reliably describe the strain states within the transition regime despite describing well the behavior of the fluid beyond the yield stress. Often, if one plots the evolution of the shear stress as a function of the shear rate in linear scale (Fig. 4a) one loses a lot of detail for the low values of the shear rate. In the case of Carbopol 990, the Herschel–Bulkley model appeared to be in good agreement with the experimental points over the entire range of shear rates. However, this was not the case for low shear rates as shown by the plot of the flow curve in logarithmic scale (Fig. 4b). Consequently, the Herschel–Bulkley model underestimated the value of the yield stress because it took into consideration all the experimental points.

To remedy this, a dynamic test was used whose stress or strain scans made it possible to evaluate the value of the yield stress. Through the evolution of the storage G' and loss G'' moduli as a function of the deformation (Fig. 5a), it was observed that at low stress and in a linear regime, the yield stress fluid was essentially elastic with $G' >> G''$. When the stress increased, the fluid left its linear regime accompanied by a decrease in G' and an increase in G''. The stress value that corresponded to the crossing point of the two curves was identified as a yield stress. It was then observed that the loss modulus became greater than the storage modulus $G'' >> G'$, and the material became liquid.

Once the yield stress was determined, the two other rheological parameters involved in the Herschel–Bulkley

Fig. 3. Anton Paar MCR 302 type rheometer with measurement systems.

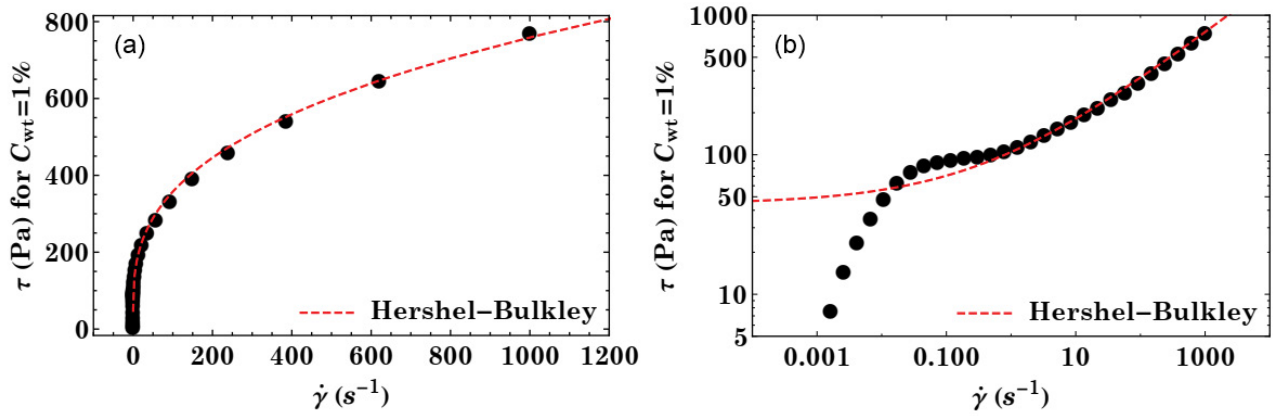

Fig. 4. Flow curves of an aqueous solution of Carbopol 990 neutralized and modeled by the Herschel–Bulkley model. (a) Linear and (b) logarithmic scale representation.

model (*k*,*n*) were identified. Three distinct deformation regimes consistent with previous macro-rheological studies [12–28] were observed. For low values of applied stress, the variation of the strain rate of the material $\dot{\gamma}$ with the applied stress was negligible. This corresponded to a solid-like behavior of the material [region (S) in Fig. 5b]. For high values of applied stress (beyond the yield stress), the material became completely liquid [region (F) in Fig. 5b] and its behavior followed the Herschel–Bulkley model (red line on Fig. 5b). For intermediate values of the applied stresses, the solid-fluid transition was not direct and the behavior of the material corresponded neither to a solid-like regime nor to a viscous flow regime [region (S + F) of Fig. 5b].

3.2. Modelling

It was necessary to search for a rheological model to explain the rheological behavior of the polymer and to determine explicit laws of behavior with a view to subsequent applications. To compare the different models likely to correctly represent the solution used, statistical quantities were employed such as the dispersion, the Theil coefficient, and the Pearson coefficient. Furthermore, to describe the behavior of the fluid, the rheological models presented in Table 1 were utilized. The dispersion is given by Eq. (1):

$$D_i = \frac{1}{N}\sqrt{\sum_{i=1}^{N}\left(\frac{\tau_{i-\text{pre}} - \tau_{i-\text{mes}}}{\tau_{i-\text{mes}}}\right)^2} \tag{1}$$

where $\tau_{i\text{-pre}}$ is the stress value predicted by the model, $\tau_{i\text{-mes}}$ the measured stress value, and N is the number of experimental points. It represented the sum of the relative mean square errors, it allowed for knowing the precision made on the adjustment of the experimental points by the models used. The model which gave the lowest value of the dispersion was the most appropriate. The second statistical quantity employed was the Theil coefficient [Eq. (2)]:

$$T_e = \frac{\sqrt{\frac{1}{N}\sum_{i=1}^{N}\left(\tau_{i-\text{pre}} - \tau_{i-\text{mes}}\right)^2}}{\sqrt{\frac{1}{N}\sum_{i=1}^{N}\tau_{i-\text{mes}}^2} - \sqrt{\frac{1}{N}\sum_{i=1}^{N}\tau_{i-\text{pre}}^2}} \tag{2}$$

It can be decomposed into three elements whose sum was equal to unity; the part of the systematic forecast

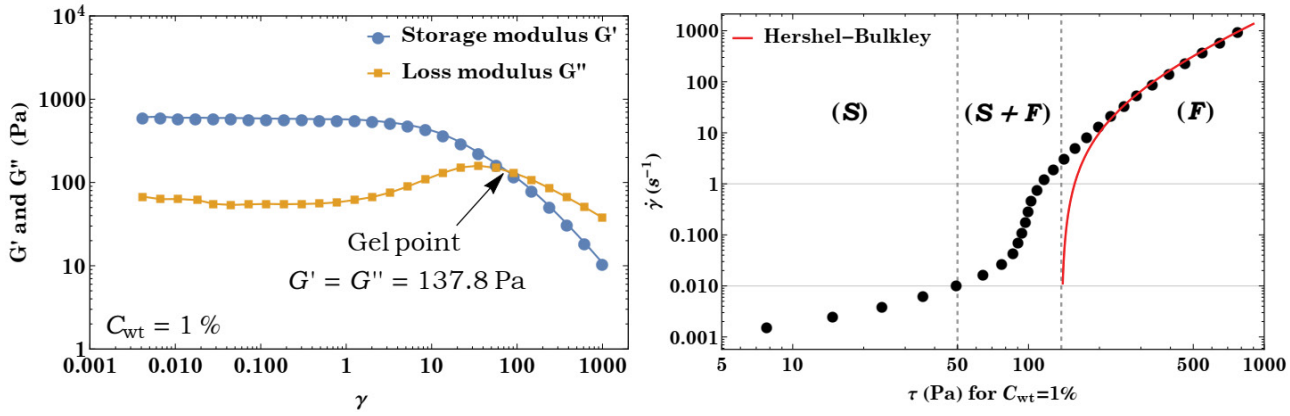

Fig. 5. (a) *G*′ and *G*″ as a function of strain in an oscillatory strain sweep test. (b) Dependence of $\dot{\gamma}$ on the applied stress τ. The red line represents the Herschel–Bulkley model which gives τ_0 = 137.8 Pa; k = 19.16 Pa·s^n; n = 0.51.

Table 1
Rheological models used to describe our hydrogel

Model	Constitutive equation	Parameters
Herschel and Bulkley [29]	$\tau = \tau_0 + k\dot{\gamma}^n$	τ_0, k, n
Papanastasiou and Boudouvis [30]	$\tau = \left(\mu_p + \tau_0\left(\frac{1-e^{-mt}}{\dot{\gamma}}\right)\right)\dot{\gamma}$	τ_0, μ_p, m
Souza–Mendes [31]	$\tau = \left(\left(\tau_0 + k\dot{\gamma}^n\right)\left(\frac{1-e^{-\frac{\mu_0}{\tau_0}\dot{\gamma}}}{\dot{\gamma}}\right)\right)\dot{\gamma}$	τ_0, k, n, μ_0
Mitsoulis et al. [32]	$\tau = \tau_0\left(1-e^{-m\dot{\gamma}}\right) + k\dot{\gamma}^n$	τ_0, k, n, m

error attributable to the difference of the mean of the predicted and measured values, the part of the forecast error due to the structure of the model, and the part of the forecast error which was residual. The most appropriate model was the one that corresponded to a very low Theil coefficient. The third statistical descriptor, which was the Pearson coefficient, was given by Eq. (3):

$$R = \frac{\sum_{i=1}^{N}\left(\tau_{i-\text{mes}} - \tau_{i-\text{pre}}\right) - \sum_{i=1}^{N}\tau_{i-\text{mes}}\sum_{i=1}^{N}\tau_{i-\text{mes}}}{\sqrt{\left[\sum_{i=1}^{N}\tau_{i-\text{mes}}^{2} - \left(\sum_{i=1}^{N}\tau_{i-\text{mes}}^{2}\right)^{2}\right] - \left[\sum_{i=1}^{N}\tau_{i-\text{pre}}^{2} - \left(\sum_{i=1}^{N}\tau_{i-\text{pre}}\right)^{2}\right]}} \quad (3)$$

It is a statistical index that expresses the intensity and direction of the linear relationship between two quantitative variables. It assumes values in the range, which goes from –1 to +1. A value of R equal to –1 or +1 indicates the existence of a perfect (functional) linear relationship between the two variables. On the other hand, this coefficient is zero ($R = 0$) when there is no linear relationship between the variables. The intensity of the linear relationship will therefore be all the stronger as the value of the coefficient is close to +1 or –1, and all the weaker as it is close to 0. The choice of the model was based on the consideration of the three descriptors at the same time.

Table 2 shows that the Mitsoulis model and that of Souza–Mendes were the most appropriate to describe the behavior of the polymer and Fig. 6a clearly shows it from which the curves of Mitsoulis and Souza–Mendes were seen to pass by many experimental points. It remained to choose between these two models. To do this, the flow curve was plotted for lower concentrations of Carbopol 990 (Fig. 6b). As can be seen from this curve, the Souza–Mendes model best described the evolution of stresses as a function of shear rates.

3.3. Concentration effect

One can recall that the constitutive equation of the rheological state of Souza–Mendes is given by Eq. (4):

$$\tau = \left(\left(\tau_0 + k\dot{\gamma}^n\right)\left(\frac{1 - e^{\frac{-\mu_0}{\tau_0}\dot{\gamma}}}{\dot{\gamma}}\right)\right)\dot{\gamma} \quad (4)$$

It is a four-parameter law: τ_0 the yield stress of the fluid, K its consistency, n its structure index, and μ_0 its initial viscosity (for low shear rates). The influence of the concentration of the polymer on these four rheological parameters was assessed.

The yield stress of the hydrogel increased with the concentration of the polymer in two different ways, for $C_{wt} \leq 0.3\%$ the yield stress was proportional to the cube of the concentration $\tau_0 \propto C_{wt}^3$, and for $C_{wt} \geq 0.3\%$ the yield stress dependence at concentration changed to $\tau_0 \propto C_{wt}^{0.6}$. The influence of the concentration was greater in the interval $C_{wt} \in [0\%–0.3\%]$ (Fig. 7a). In the same concentration interval, the initial viscosity of the fluid increased very rapidly to reach a limiting value which would change slightly for concentrations larger than $C_{wt} = 0.3\%$ (Fig. 7b).

Similarly, the evolution of the consistency k and the structure index n of the studied fluid were plotted as a function of the concentration of the polymer (Fig. 8). The concentration had a consistency amplifying effect in

Table 2
Values of statistical descriptors for the four models

	Herschel and Bulkley	Papanastasiou and Boudouvis	Mitsoulis	Souza–Mendes
Dispersion D_i	24.82	13.87	2.98	3.36
Theil's coefficient T_i	0.0401	0.1508	0.04277	0.0424
Pearson's coefficient R	0.996238	0.9484	0.996386	0.996447

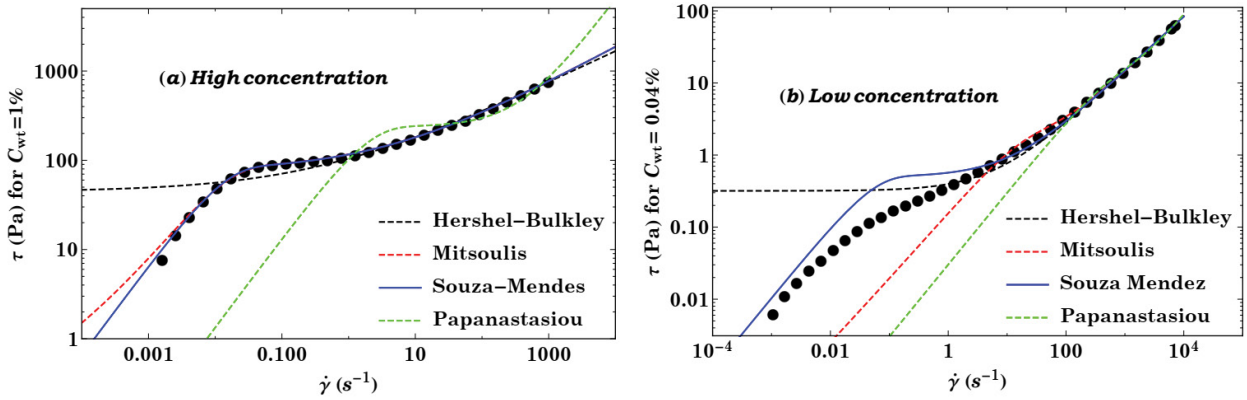

Fig. 6. (a) Flow curve of an aqueous solution of Carbopol 990 with a concentration C_{wt} = 1% neutralized and modeled by four constitutive equations and (b) same flow curve for a lower concentration C_{wt} = 0.04%.

the interval C_{wt} ϵ (0%–0.3%) and the consistency varied in the power of four in this interval $k \propto C_{wt}^{4}$ (Fig. 8a). For concentrations larger than C_{wt} = 0.3%, the increase in consistency was a root function of concentration $k \propto C_{wt}^{0.5}$. This indicated that the consistency of the fluid was sensitive over the whole range of concentrations but much more for concentrations less than or equal to C_{wt} = 0.3%. Likewise, the variation of structure index of working fluid with concentration is shown in Fig. 8b. In contrast to consistency, the structure index of the test fluid decreased with increasing polymer concentration. This decrease was very acute for concentrations lower than C_{wt} = 0.3%, then the variation of the structure index was very low for $C_{wt} \geq 0.3\%$.

3.4. pH effect

To quantify the influence of pH on the rheological parameters of the constitutive Souza–Mendes equation, several rheological tests were performed which allow for the determination of these parameters for different pH at a constant polymer concentration C_{wt} = 0.1%. In Fig. 9a, the evolution of the yield stress τ_0 as a function of pH are presented. An interesting behavior was observed for the yield stress.

For a low pH the fluid behaved like a Newtonian and the yield stress was almost zero. Then, by increasing the pH, the yield stress increased and reached its maximum value in the neutral zone and the fluid became non-Newtonian of viscoplastic type. A decrease was noticed in the yield stress when entering the basic zone and again the fluid became Newtonian for high pH values.

The initial viscosity is shown in Fig. 9b as a function of pH. The same evolution as that of the yield stress was observed. To know the influence of pH on the consistency of the fluid, the variation of k is represented in Fig. 10a. An evolution in the form of a Gaussian was observed which confirmed the Newtonian character in acidic and basic media and the non-Newtonian character in neutral medium. This deduction was ensured by the evolution of the structure index in Fig. 10b in which the observed values were close to unity n = 1 for low and high pH, and the two branches tended towards a value of n = 0.5 in the interval pH ϵ (6–10).

3.5. Temperature effect

Knowledge of the effect of temperature on the physical and rheological properties of the solution is fundamental in pharmaceutical and industrial processes. Failure to maintain

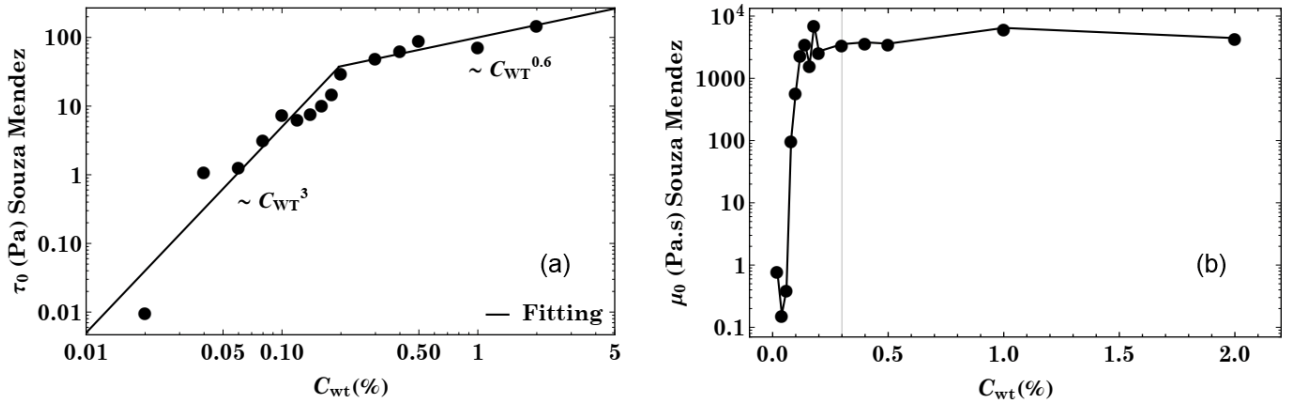

Fig. 7. (a) Evolution of the yield stress as a function of the concentration of the polymer for a neutral pH and (b) evolution of the initial viscosity as a function of the concentration of the polymer for a neutral pH.

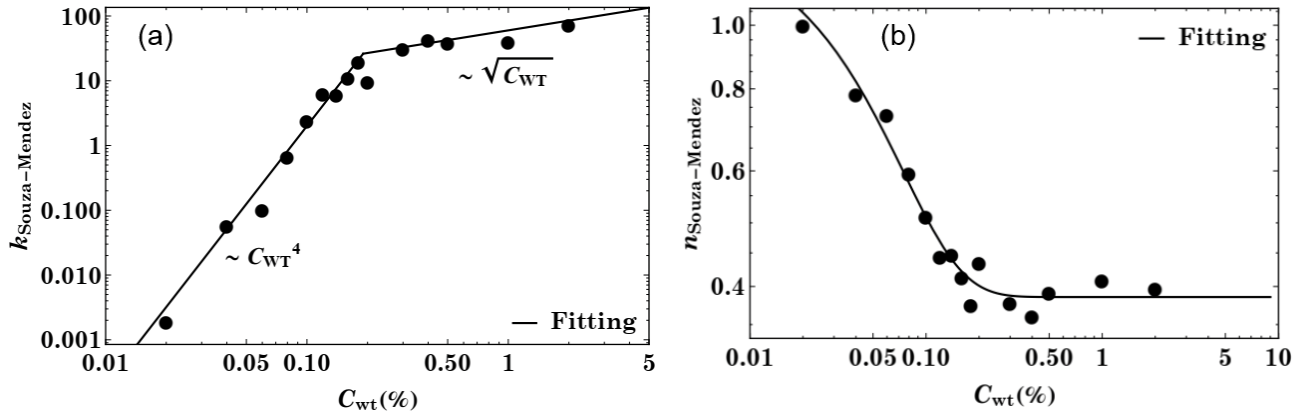

Fig. 8. (a) Evolution of the consistency of the fluid according to the concentration for a neutral pH and (b) evolution of the structure index according to the concentration of the polymer.

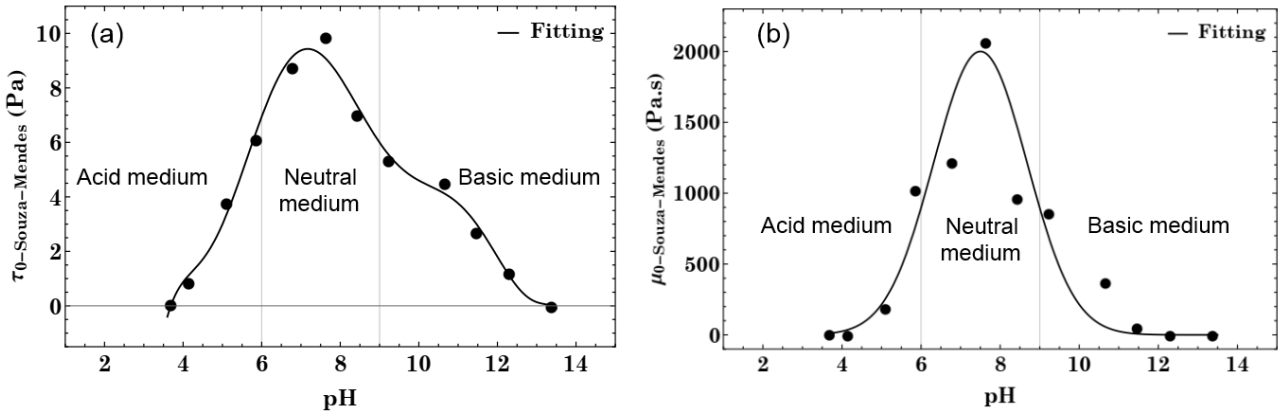

Fig. 9. (a) Evolution of the yield stress as a function of pH for a concentration C_{wt} = 0.1% and (b) evolution of the initial viscosity as a function of pH for the same concentration.

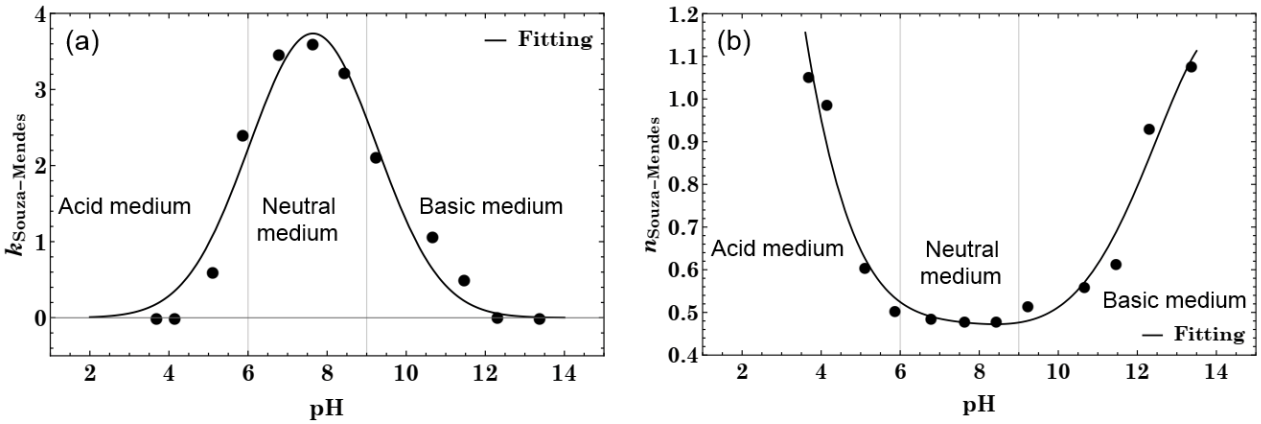

Fig. 10. (a) Evolution of fluid consistency as a function of pH for a concentration C_{wt} = 0.1% and (b) evolution of the structure index as a function of pH for the same concentration.

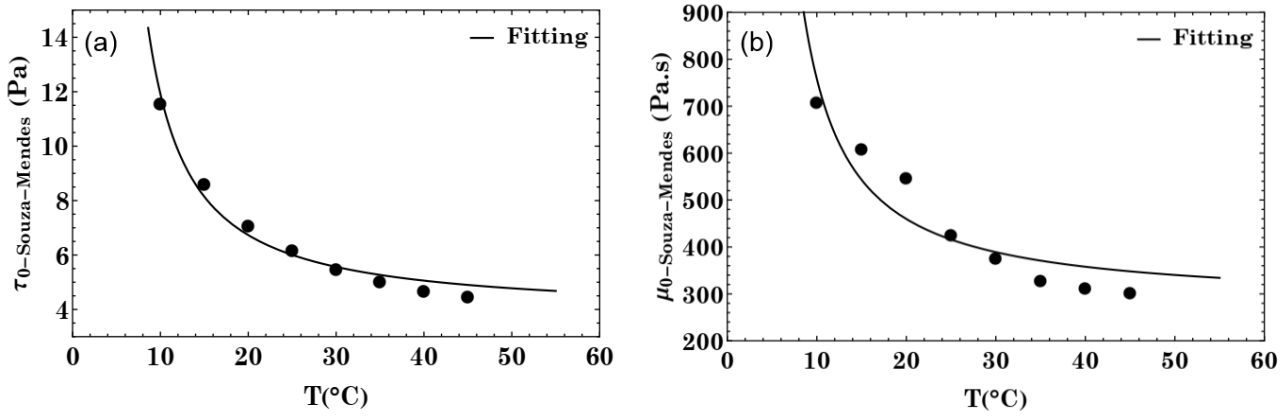

Fig. 11. (a) Evolution of the yield stress as a function of the temperature for a concentration C_{wt} = 0.1% and pH ≈ 7 and (b) evolution of the initial viscosity as a function of the temperature for the same concentration and the same pH.

a constant temperature during measurement readings in an experiment considerably affects the intrinsic values and gives completely erroneous interpretations of the obtained results. Consequently, the temperature must be imposed and kept constant for the duration of the measurements.

Fig. 11 shows the evolution of two rheological parameters (τ_0, μ_0) as a function of temperature. The two parameters showed the same evolution as represented by an exponential decrease. For the initial viscosity (Fig. 11b), the solid line represented the Arrhenius law which did

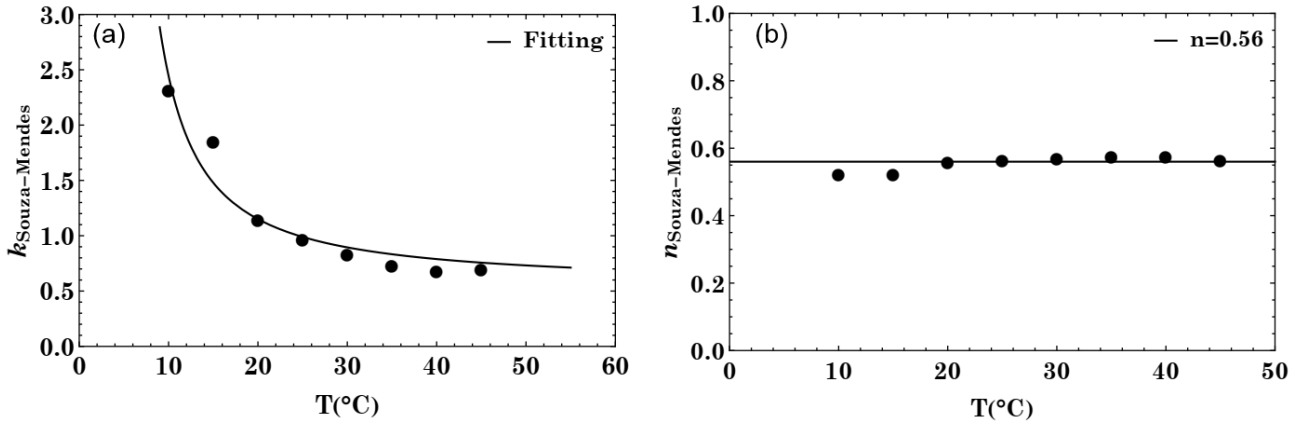

Fig. 12. Evolution of consistency in (a) and the structure index (b) as a function of for a concentration C_{wt} = 0.1% and a neutral pH.

not describe well the evolution of the initial viscosity. This was due to the non-Newtonian nature of the polymer.

Quantifying the influence of temperature on the other two rheological parameters *k*,*n*, was also crucial. Therefore their variations were plotted as a function of temperature in Fig. 12. It was observed that the structure index was not really affected by the change in temperature in the range (10°C–45°C) as shown in Fig. 12b. On the other hand, the consistency of the fluid was influenced by the temperature over the whole range before reaching a constant plateau and did not vary after T = 35°C.

3.6. Discussion

In this study, competing effects of pH and concentration on the rheological properties of Carbopol 990 were observed. This was evidenced by the peaks as a function of pH. These rheology changes were likely related to changes in the underlying gel microstructure. It was known from previous studies with small angle light scattering that when ions were added, polymers swelled significantly, up to three times orders of magnitude in volume [33]. These swollen particles occupied a larger volume fraction, which increased the interference effects and made the sample more like an elastic solid. The particles got bigger and bigger with the base titration until they had no space to expand and compressed against each other. Once the ions inside the particles were completely dissociated, the particles began to experience a net inward osmotic pressure, causing them to compress. Several key rheological quantities that were examined seemed to be intimately related to particle size and volume fraction. The observed behavior was consistent with a model of particle size and volume fractions changing with pH and concentration. At low pH, the unmodified polymers were tightly bound and did not fill the space. However, evidence of yield stress even at these low concentrations indicated that the suspension had some sort of mesostructure that spanned the sample. The most probable structure was that of a percolated network and the rheology supported this image. In a recent study two distinct regions of tracer particle mobility were observed in samples at these concentrations, indicating that there were solvent pools within a percolated gel network [33].

The current data showed the highest values of yield stress at intermediate pH values for the concentration. This trend of increasing yield stress with increasing concentration at constant pH supported the idea of a blocking effect due to higher volume fraction at higher pH. The compression of the elastic particles led to a very strongly wedged structure, as evidenced by the high yield stresses and the consistencies observed in this regime. This was because the particles were tightly packed and did not easily move relative to each other or rearrange. Instead, they dissipated disturbances elastically by deforming. The compression of the elastic particles led to a strongly clamped structure, as evidenced by the high yield stresses in this regime. At high pH, osmotic effects could lead to particle deflation. It was believed that this swelling was not as drastic as the initial swelling. The particles did not return to their initial size. Rather, this slight shrinkage simply led to a loosening of the structure, or a lowering of the compression between the particles, and thus allowed for greater movement of the particles in response to disturbances. Strong concentration effects were also observed. Lower concentration samples were likely to reach the gap filling limit much later than higher concentration samples. These samples eventually remained in the form of percolated networks, at neutral pH, while the samples with higher concentration quickly became strong compressed networks.

4. Conclusions

The characterization protocol developed in this work made it possible to identify and choose the model that best suited the fluid used in this experimental study. Based on dispersion, Theil's coefficient, and Pearson's coefficient as evaluation criteria, and even on the graphical adjustment of the experimental points by the five models used; the choice fell on the four-parameter Souza–Mendes model. This model adequately translated the evolution of the non-Newtonian character of the viscoplastic hydrogel over a wide range of shear rates.

The Carbopol 990 gel exhibited a non-Newtonian behavior of viscoplastic type and its rheological state was well described by the Souza–Mendes model. The polymer concentration had an amplifying effect on the yield stress and

the initial viscosity of the fluid maintained at a neutral pH. Similarly, the consistency of the fluid increased with the concentration but the structure index decreased until it reached a limit value of the order of n = 0.38. The yield stress and the initial viscosity had a maximum values in the neutral zone pH ϵ (6–9), and low values in acidic and basic media. The evolution had a form of a Gaussian function for the initial viscosity. The same was seen for the consistency which was maximum in a neutral medium and tended towards low values outside this zone. On the other hand, the index of structure behaved inversely because its maximum value was in acidic and basic mediums $n \approx 1$, and its minimum value in neutral medium. Direct proof was provided that Carbopol 990 behaved as a Newtonian fluid in acidic and basic media and strongly non-Newtonian in neutral media. Increasing the temperature decreased the yield stress, the initial viscosity, and even the consistency in the range T ϵ (10°C–45°C). On the other hand, the structure index of the polymer was not affected by this increase and remained practically unchanged. In closing although a lot of information about the rheological behavior of Carbopol has been generated, much of its underlying structure remains a mystery, which needs to be further investigated.

References

[1] H.A. Barnes, K. Walters, The yield stress myth?, Rheol. Acta, 24 (1985) 323–326.
[2] H.A. Barnes, The yield stress—a review or 'παντα ρει'—everything flows?, J. Non-Newtonian Fluid Mech., 81 (1999) 133–178.
[3] G. Astarita, Letter to the editor: the engineering reality of the yield stress, J. Rheol., 34 (1990) 275, doi: 10.1122/1.550142.
[4] J.P. Hartnett, R.Y.Z. Hu, Technical note: the yield stress—an engineering reality, J. Rheol., 33 (1989) 671–679.
[5] I.D. Evans, Letter to the editor: on the nature of the yield stress, J. Rheol., 36 (1992) 1313–1321.
[6] Q.D. Nguyen, D.V. Boger, Measuring the flow properties of yield stress fluids, Annu. Rev. Fluid Mech., 24 (1992) 47–88.
[7] P.C.F. Møller, J. Mewis, D. Bonn, Yield stress and thixotropy: on the difficulty of measuring yield stresses in practice, Soft Matter, 2 (2006) 274–283.
[8] P.C.F. Møller, A. Fall, D. Bonn, Origin of apparent viscosity in yield stress fluids below yielding, Europhys. Lett., 87 (2009) 38004, doi: 10.1209/0295-5075/87/38004.
[9] N.J. Balmforth, I.A. Frigaard, G. Ovarlez, Yielding to stress: recent developments in viscoplastic fluid mechanics, Annu. Rev. Fluid Mech., 46 (2014) 121–146.
[10] J.O. Carnali, M.S. Naser, The use of dilute solution viscometry to characterize the network properties of Carbopol microgels, Colloid. Polym. Sci., 270 (1992) 183–193.
[11] E.M. Ahmed, Hydrogel: preparation, characterization, and applications: a review, J. Adv. Res., 6 (2015) 105–121.
[12] A.M.V. Putz, T.I. Burghelea, The solid–fluid transition in a yield stress shear thinning physical gel, Rheol. Acta, 48 (2009) 673–689.
[13] J.M. Piau, Carbopol gels: elastoviscoplastic and slippery glasses made of individual swollen sponges: meso- and macroscopic properties, constitutive equations and scaling laws, J. Non-Newtonian Fluid Mech., 144 (2007) 1–29.
[14] J.-Y. Kim, J.-Y. Song, E.-J. Lee, S.-K. Park, Rheological properties and microstructures of Carbopol gel network system, Colloid. Polym. Sci., 281 (2003) 614–623.
[15] B.W. Barry, M.C. Meyer, The rheological properties of Carbopol gels I. Continuous shear and creep properties of Carbopol gels, Int. J. Pharm., 2 (1979) 1–25.
[16] M.T. Islam, N. Rodríguez-Hornedo, S. Ciotti, C. Ackermann, Rheological characterization of topical carbomer gels neutralized to different pH, Pharm. Res., 21 (2004) 1192–1199.
[17] E. Di Giuseppe, F. Corbi, F. Funiciello, A. Massmeyer, T.N. Santimano, M. Rosenau, A. Davaille, Characterization of Carbopol® hydrogel rheology for experimental tectonics and geodynamics, Tectonophysics, 642 (2015) 29–45.
[18] P. Moller, A. Fall, V. Chikkadi, D. Derks, D. Bonn, An attempt to categorize yield stress fluid behaviour, Philos. Trans. R. Soc. London, Ser. A, 367 (2009) 5139–5155.
[19] P. Coussot, L. Tocquer, C. Lanos, G. Ovarlez, Macroscopic vs. local rheology of yield stress fluids, J. Non-Newtonian Fluid Mech., 158 (2009) 85–90.
[20] R.J. Ketz Jr., R.K. Prud'homme, W.W. Graessley, Rheology of concentrated microgel solutions, Rheol. Acta, 27 (1988) 531–539.
[21] M.K.N. Ambuter, Polymeric Stabilizers for Liquid Detergents, K.-Y. Lai, Ed., Liquid Detergents, 2nd ed., CRC Press, Piscataway, New Jersey, U.S.A., 2005.
[22] J. Ricka, T. Tanaka, Swelling of ionic gels: quantitative performance of the Donnan theory, Macromolecules, 17 (1984) 2916–2921.
[23] T. Burghelea, Transport Phenomena in Viscoplastic Materials, V.B. Teodor Burghelea, Ed., Transport Phenomena in Complex Fluids, Springer, Cham, 2019, pp. 167–258.
[24] T. Divoux, D. Tamarii, C. Barentin, S. Manneville, Transient shear banding in a simple yield stress fluid, Phys. Rev. Lett., 104 (2010) 208301, doi: 10.1103/PhysRevLett.104.208301.
[25] T. Burghelea, M. Moyers-Gonzalez, R. Sainudiin, A non-linear dynamical system approach for the yielding behaviour of a viscoplastic material, Soft Matter, 13 (2017) 2024–2039.
[26] E. Weber, M. Moyers-González, T.I. Burghelea, Thermorheological properties of a Carbopol gel under shear, J. Non-Newtonian Fluid Mech., 183 (2012) 14–24.
[27] M. Moyers-Gonzalez, T.I. Burghelea, J. Mak, Linear stability analysis for plane-Poiseuille flow of an elastoviscoplastic fluid with internal microstructure for large Reynolds numbers., J. Non-Newtonian Fluid Mech., 166 (2011) 515–531.
[28] E. Younes, V. Bertola, C. Castelain, T. Burghelea, Slippery flows of a Carbopol gel in a microchannel, Phys. Rev. Fluids, 5 (2020) 083303, doi: 10.1103/PhysRevFluids.5.083303.
[29] W.H. Herschel, R. Bulkley, Konsistenzmessungen von Gummi-Benzollösungen, Kolloid-Zeitschrift, 39 (1926) 291–300.
[30] T.C. Papanastasiou, A.G. Boudouvis, Flows of viscoplastic materials: models and computations, Comput. Struct., 64 (1997) 677–694.
[31] P.R.S. Mendes, E.S.S. Dutra, Viscosity function for yield-stress liquids, Appl. Rheol., 14 (2004) 296–302.
[32] E. Mitsoulis, S.S. Abdali, N.C. Markatos, Flow simulation of Herschel–Bulkley fluids through extrusion dies, Can. J. Chem. Eng., 71 (1993) 147–160.
[33] F.K. Oppong, J.R. de Bruyn, Mircorheology and jamming in a yield-stress fluid, Rheol. Acta, 50 (2011) 317–326.